

Article

Performance Analysis of Cooperative Low-Power Wide-Area Network for Energy-Efficient B5G Systems

Chang Seok You ^{1,2}, Jeong Seon Yeom ² and Bang Chul Jung ^{2,*}¹ Agency for Defense Development, Daejeon 34186, Korea; cs_you@add.re.kr² Department of Electronics Engineering, Chungnam National University, Daejeon 34134, Korea; jsyeom@cnu.ac.kr

* Correspondence: bcjung@cnu.ac.kr; Tel.: +82-42-821-6580

Received: 24 March 2020; Accepted: 20 April 2020; Published: 22 April 2020



Abstract: Low-power wide-area networks (LPWANs) have received extensive attention from both academia and industry, since they can efficiently provide massive connectivity to internet of things (IoT) devices in wide geographical areas with low cost and low power consumption. Recently, it was shown that macro-diversity among multiple gateways significantly improves the performance of uplink LPWANs by coherently combining multiple received signals at gateways. We call such networks *cooperative* LPWANs. In this paper, the error performance of an uplink cooperative LPWAN is mathematically analyzed in terms of outage probability, bit error rate (BER), and diversity order. It is assumed that there exist multiple (two or more) gateways that have multiple antennas and are located at arbitrary positions in the LPWAN area. Each gateway exploits the optimal maximum-ratio combining (MRC) technique to decode the received signal, and then the signals after MRC are delivered to the cloud fusion center for coherent combining in the cooperative LPWAN. The main results, the closed-form expressions of outage probability and BER, were derived by utilizing the *hyper-Erlang* distribution. Furthermore, the macro-diversity order was mathematically derived. The mathematical analysis was validated through extensive computer simulations. It worth noting that the mathematical analysis of the error performance of cooperative LPWANs is the first theoretical result in the literature to the best of our knowledge.

Keywords: low-power wide-area network (LPWAN); cooperative communication; macro-diversity; bit-error-rate (BER); outage probability; diversity order

1. Introduction

The low-power wide-area network (LPWAN) is a promising wireless platform to meet three key requirements of IoT applications distributed over wide areas; i.e., low cost, large scale deployment, and high energy efficiency. Most of all, it can be supported on battery-powered electronic devices for 10-years while communicating at low data-rates to gateways several kilometers away. It is conceived as an appealing technology to realize smart cities, smart farms, and smart buildings. In recent times, LPWAN has been actively researched in relation to sustainable and fully-connected IoT for ongoing 5G and towards 6G; i.e., long-term evolution (LTE) machine-type-communications (LTE-MTC), narrow band-IoT (NB-IoT), LoRa (long range), and Bluetooth low energy (BLE). LTE-MTC is an LPWA technology standard published by the 3GPP, which can achieve a much higher data rate. NB-IoT is an evolution form regular MTC to massive MTC (mMTC) which was a 3GPP standard in 2016 [1]. They all work over the licensed spectrum. LoRa operates over an unlicensed spectrum; that is, 433 MHz, 868 MHz (Europe), 915 MHz (Australia and North America), and 923 MHz (Asia). As the chip spread spectrum technology is defined by the LoRa Alliance in 2015 [2], it allows the cost of each LoRa device to be lowered with the usage of the cheap oscillator. BLE was released in 2010 as part of the Bluetooth 4.0 server's specifications [3], which works over the unlicensed 2.4 GHz band, and the transmission range

can be up to 100 m. As supported by different standards organizations and alliances, each piece of LPWA technology shows different practical deployment potential. LTE-MTC and NB-IoT may be favored by cellular network operators due to high compatibility with existing cellular networks, while LoRa and BLE are supported by IoT operators with specific applications due to their good network scalability [4]. Among the IoT networks, LPWAN is certainly becoming the main technique envisioned to be part of the cooperative distributed networks in IoT network connectivity in the ongoing 5G and towards 6G.

Recent studies have been conducted to address and analyze the performance of the LPWAN. In [5], they assess the performance of LoRaWAN—which is one of the main LPWA technology available—in terms of network performance metrics, such as range, coverage, latency, and packet delivery ratio. In [6], they derive the uplink throughput and data transmission time of a single LoRaWAN end device and analyze the maximum number of end devices which can be served by a single LoRaWAN base station. In [7], they analyze the flexibility of LoRa and propose various strategies to adapt its radio parameters to different deployment scenarios and compute the energy consumption of LoRa transceivers. In [8], they analyze the coverages and the capacities of four types of LPWAN using a real site deployment assuming traffic growth. They all explain that the LPWAN possess the ability to offer low-cost connections for a huge number of low-power devices distributed over large areas [9].

Nevertheless, the LPWAN still has several challenges to be addressed effectively, including interference management, the massive access scheme, the optimal coexistence scheme, and energy efficient schemes, which are presented with overall knowledge about LPWAN in [10].

Most of all, despite LPWAN wireless protocols enabling long-range communications (up to 10–15 km in rural zones and 2–5 km in urban zones [11]) between connected devices with minimal energy requirements (battery can last up to 10 years for low data usage cases), communications are not always guaranteed. Because it depends on data range, availability, range, noise, and required throughput [12]. Actually, devices located in urban spaces deep inside buildings will experience severe drain in the battery, as their signals are highly attenuated, even at the closest gateway (GW) [13]. In [13], the decoding weak transmission solution is presented with the use of the *coherent combining technique*, which enhances both the battery lives of client devices and the coverage of LPWANs in major urban deployments. It allows multiple LoRa wide-area network (LoRaWAN) GWs to pool their received signals in the *cloud*, coherently combining them in order to detect weak signals that are not decodable at any individual GW. It was implemented as a service running on a campus-wide LoRaWAN network installed at Carnegie Mellon University and evaluated through proof-of-concept experiments and a large-scale, trace-driven simulation. That is a coherent combining technique, which is similar to the macro-diversity technique in the cellular network. They evaluated it over a test network and through a simulation using traces from a LoRaWAN deployment. However, the performance analysis is not presented in the literature.

Actually, it is not trivial to attain tractable exact performance analysis for networks with multiple antennas. In [14], the cloud-radio access network with remote radio heads (RRHs) is analyzed in term of outage probability, for which RRHs are equipped with multiple antennas. The exact closed-form expression for the outage probability is obtained. However, It is derived from using the moment generating function approach with the approximation. With the finite limiting factor, it does not match well with the simulation result in the low signal-to-noise ratio (SNR) regime. This paper aims to exactly address the error performance analysis of the cooperative uplink LPWAN with multiple antennas GWs. The exact closed-form expressions for the performance analysis are derived using the exact channel distribution information (CDI) (*hyper-Erlang* distribution) [15]. LPWAN is basically based on the low power transmission. It is certainly needed to analyze the performance exactly in the low SNR regime. The exact closed-form expressions of bit error rate (BER) and outage probability performances are obtained. Furthermore, the diversity order is obtained from the derived BER expression, which is the first theoretical result in the literature. Finally, the asymptotic expression of BER is addressed with the numerical results.

The rest of the paper is organized as follows. The system model is explained in Section 2. In Section 3, the novel channel distribution is introduced and the analytical expressions for the error performances are derived. The numerical results are presented in Section 4. Finally, we draw conclusions in Section 5.

2. System Model

In this paper, we consider the uplink cooperative system in the LPWAN with multiple GWs. Considering a real situation and a simplification of analysis, the system consists of N GWs, which are equipped with K_i ($i \in \{1, 2, \dots, N\}$) multiple antennas in each and an IoT device (ID) with a single antenna, as shown in Figure 1. Then, the received signal at i -th GW, $\mathbf{y}_i \in \mathbb{C}^{K_i \times 1}$ ($i \in \{1, 2, \dots, N\}$), is given by

$$\mathbf{y}_i = \mathbf{h}_i \sqrt{P} d_i^{-\alpha} x + \mathbf{n}_i, \tag{1}$$

where P denotes the transmission power of the ID and d_i denotes the distance between the ID and the i -th GW. The term α denotes the path-loss exponent and x is a signal of the ID, which has a unit power; i.e., $\mathbb{E}[|x|^2] = 1$. In this paper, it is assumed that the small-scale fading channel between the ID and each GW follows a Rayleigh fading model, such as [16]. Thus, the fading channel vector from the ID to i -th GW is represented as $\mathbf{h}_i = [h_{i,1} \ h_{i,2} \ \dots \ h_{i,K_i}]^T$ and follows the identically and independently distributed (i.i.d.) complex Gaussian distribution with zero mean and unit variance; i.e., $\mathbf{h}_i \sim \mathcal{CN}(0, \mathbf{I}_{K_i})$. The additive white Gaussian noise (AWGN) at i -th GW is represented as $\mathbf{n}_i \in \mathbb{C}^{K_i \times 1}$, each element of which is identically and independently distributed complex Gaussian random variable with zero mean and variance of N_0 . It is assumed that each ID knows the local channel state information by a pilot signal from the ID. At each GW, the maximum ratio combining (MRC) is operated in order to maximize the SNR, and the minimal essential information, a real-valued combining signal, is derived to the cloud server.

$$\tilde{y}_i = \sqrt{d_i^{-\alpha}} \mathbf{h}_i^H \mathbf{y}_i = \sqrt{P} d_i^{-\alpha} \|\mathbf{h}_i\|^2 x + \tilde{n}_i, \tag{2}$$

where $\tilde{n}_i \sim \mathcal{CN}(0, d_i^{-\alpha} \|\mathbf{h}_i\|^2)$ is related to the additive white Gaussian noise term. The cloud server receives the essential information from multiple GWs and then combines them as follows:

$$\tilde{y} = \frac{1}{\sqrt{\sum_{i=1}^N d_i^{-\alpha} \|\mathbf{h}_i\|^2}} \sum_{i=1}^N \tilde{y}_i = \sqrt{P \sum_{i=1}^N d_i^{-\alpha} \|\mathbf{h}_i\|^2} x + \tilde{n}, \tag{3}$$

where $\tilde{n} \sim \mathcal{CN}(0, N_0)$.

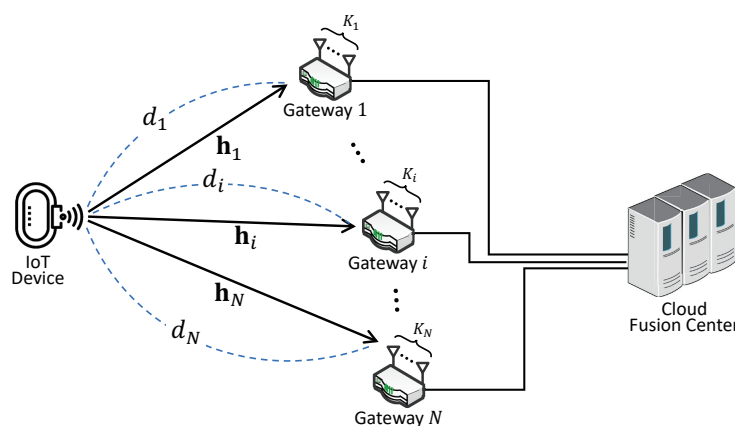


Figure 1. Uplink cooperative technique in a low-power wide-area network (LPWAN) with multiple antenna gateways (GWs).

3. Error Performance Analysis

In order to derive the error probabilities, we first should know a distribution of effective channel gain for a signal at the cloud server. The effective channel gain, Z , is equal to

$$Z = \sum_{i=1}^N Z_{\gamma_i}^{K_i} = \sum_{i=1}^N d_i^{-\alpha} \|\mathbf{h}_i\|^2, \tag{4}$$

where $\gamma_i = d_i^{-\alpha}$ ($i \in \{1, \dots, N\}$). Since the fact is that $Z_{\gamma_i}^{K_i}$ follows the Erlang distribution with $K_i\gamma_i$ mean and $K_i\gamma_i^2$ variance represented as following probability density function (p.d.f.):

$$f_{Z_{\gamma_i}^{K_i}}(z) = \frac{z^{K_i-1}}{(K_i - 1)! \gamma_i^{K_i}} e^{-\frac{z}{\gamma_i}}. \tag{5}$$

the distribution of the effective channel gain Z is the same as the distribution of the sum of N *non-identical* and independent random variables, which follows Erlang distribution. It is known as hyper-Erlang distribution [15] which is the mixture of N mutually independent Erlang distribution and parallel N -phase Erlang distribution weighted with probabilities. Therefore, the p.d.f. of Z is given by

$$f_Z(z) = \sum_{i=1}^N \sum_{j=1}^{K_i} A_{ij} f_{Z_{\gamma_i}^j}(z). \tag{6}$$

The coefficient A_{ij} is iteratively obtained by the recursive method [15]. See Appendix A.

3.1. Outage Probability

From the definition of outage probability, it is straightforward to calculate the outage probability. Generally, an outage occurs when the channel capacity defined $\log(1 + \text{SNR})$ is below the target rate R [17].

In non-cooperative LPWAN, the outage probability at the GW i is given from (2) as follows.

$$P_{o,i} = \Pr \left\{ \log \left(1 + Z_{\gamma_i}^{K_i} \frac{P}{N_0} \right) < R \right\} = \Pr \left\{ Z_{\gamma_i}^{K_i} < \frac{2^R - 1}{\rho} \right\} = \Pr \left\{ Z_{\gamma_i}^{K_i} < R' \right\}, \tag{7}$$

where $\rho = P/N_0$ denotes the SNR and $R' := (2^R - 1)/\rho$ is the outage channel threshold related to the target rate. Note that the cumulative distribution function (c.d.f.) of Erlang distribution $Z_{\gamma_i}^{K_i}$ for all i is given as $F_{Z_{\gamma_i}^{K_i}}(z) = 1 - e^{-z\gamma_i^{-1}} \sum_{K=0}^{K_i-1} \frac{z^K \gamma_i^{-K}}{K!}$. Therefore, the outage probability $P_o(i, K_i)$ is derived as

$$P_o(i, K_i) = \Pr \left\{ Z_{\gamma_i}^{K_i} < R' \right\} = F_{Z_{\gamma_i}^{K_i}}(R') = 1 - e^{-R'\gamma_i^{-1}} \sum_{K=0}^{K_i-1} \frac{(R')^K \gamma_i^{-K}}{K!}. \tag{8}$$

Considering the effective channel gain of the uplink cooperation, the outage probability of that is given as follows

$$P_o = \Pr \{ Z < R' \}, \tag{9}$$

Since the hyper-Erlang distribution is given as the sum of N polynomials, which are the K_i polynomials of the product of the coefficient A_{ij} and the p.d.f. of each Erlang distributions as j is the antenna index, the cumulative distribution function (c.d.f.) of hyper-Erlang distribution is obtained from the summation of N Erlang distributions c.d.f as follows.

$$F_Z(z) = \int_0^z \sum_{i=1}^N \sum_{j=1}^{K_i} A_{ij} f_{Z_{\gamma_i}^j}(y) dy = \sum_{i=1}^N \sum_{j=1}^{K_i} A_{ij} \int_0^z f_{Z_{\gamma_i}^j}(y) dy = \sum_{i=1}^N \sum_{j=1}^{K_i} A_{ij} F_{Z_{\gamma_i}^j}(z). \tag{10}$$

Therefore, the outage probability of the uplink cooperative system in LPWAN is exactly derived as follows:

$$P_o = \Pr \{Z < R'\} = F_Z (R') = \sum_{i=1}^N \sum_{j=1}^{K_i} A_{ij} F_{Z_{\gamma_i}^j} (R') = \sum_{i=1}^N \sum_{j=1}^{K_i} A_{ij} P_o(i, j). \tag{11}$$

3.2. Bit Error Rate (BER)

In this subsection, we derive the BER of the uplink cooperative technique in LPWAN. First, we assume that the transmit signal of the ID is modulated to quadrature phase-shift keying (QPSK) modulation. The BER of QPSK modulation is known as $Q(\sqrt{\text{SNR}})$.

From (2), the conditional BER for given channel gain $\|\mathbf{h}_i\|$ at the GW i in non-cooperative LPWAN is given as

$$\Pr(\mathcal{E}_{b,i} \mid \|\mathbf{h}_i\|) = Q \left(\sqrt{d_i^{-\alpha} \|\mathbf{h}_i\|^2 \rho} \right), \tag{12}$$

where $\mathcal{E}_{b,i}$ dedicates the bit-error event at GW i . We easily can derive the non-cooperative BER of the i -th GW with K_i antennas as follows:

$$\begin{aligned} P_b(i, K_i) &\triangleq \Pr(\mathcal{E}_{b,i}) = \mathbb{E}_{\|\mathbf{h}_i\|} \left[Q \left(\sqrt{d_i^{-\alpha} \|\mathbf{h}_i\|^2 \rho} \right) \right] \\ &= \int_0^\infty Q(\sqrt{z\rho}) f_{Z_{\gamma_i}^{K_i}}(z) dz \stackrel{(a)}{=} \frac{1}{2} \left(1 - \sum_{k=0}^{K_i-1} \binom{2k}{k} \frac{(2\gamma_i + 4)^{-k}}{\sqrt{1 + 2/\gamma_i}} \right), \end{aligned} \tag{13}$$

where (a) is given in [18].

Now, we analyze the BER of the uplink cooperative technique. As in Equation (12), The conditional BER for given all channel gains, $\forall \|\mathbf{h}_i\|$ at the cloud server is given as

$$\Pr(\mathcal{E}_b \mid \forall \|\mathbf{h}_i\|) = Q \left(\sqrt{\sum_{i=1}^N d_i^{-\alpha} \|\mathbf{h}_i\|^2 \rho} \right), \tag{14}$$

where \mathcal{E}_b dedicates the bit-error event at the cloud server.

Finally, we can obtain the exact closed-form BER performance of the uplink cooperative technique in the presence of the cloud server connected with them as follows.

$$\begin{aligned} P_b &= \mathbb{E}_{\forall \|\mathbf{h}_i\|} \left[Q \left(\sqrt{\sum_{i=1}^N d_i^{-\alpha} \|\mathbf{h}_i\|^2 \rho} \right) \right] = \int_0^\infty Q(\sqrt{z\rho}) f_Z(z) dz = \int_0^\infty Q(\sqrt{z}) \sum_{i=1}^N \sum_{j=1}^{K_i} A_{ij} f_{Z_{\gamma_i}^j}(z) dz \\ &= \sum_{i=1}^N \sum_{j=1}^{K_i} A_{ij} \int_0^\infty Q(\sqrt{z}) f_{Z_{\gamma_i}^j}(z) dz = \sum_{i=1}^N \sum_{j=1}^{K_i} A_{ij} P_b(i, j). \end{aligned} \tag{15}$$

3.3. Diversity Order

In this section, we analyze the diversity order of the uplink cooperative technique with the exact BER expression (Equation (15)), which is defined as:

$$\eta = - \lim_{\rho \rightarrow \infty} \frac{\log_{10} P_b}{\log_{10} \rho}, \tag{16}$$

which is used to verify the tendency of BER performance; i.e., the slope of BER curve, in high SNR regime [17]. The diversity order is obtained through Taylor series expansion for (15), of which the first-order coefficient shows how the system parameters affect the performance in high SNR regime;

e.g., the distances between ID and GWs, the number of antennas, pass-loss factor, and so on. An asymptotic expression is given by

$$P_b \approx \beta_b \rho^{-K} = \frac{\Psi}{2^K} \prod_{i=1}^N d_i^{\alpha K_i} \rho^{-K}, \tag{17}$$

Proof: See Appendix B.

where $\Psi = \binom{2K-1}{K-1}$, $K = \sum_{i=1}^N K_i$, and β_b denotes the first coefficient of Taylor series expansion for the BER. It varies according to the total number of antennas of all GWs that participate in cooperative communication. It also depends on the distances between the ID and the GWs. Plugging (17) into (16) shows that the diversity order of uplink cooperative LPWAN system with N GWs equipped with multiple antennas K_i is equal to K ; i.e.,

$$\eta = - \lim_{\rho \rightarrow \infty} \frac{\log_{10} \left(\frac{\Psi}{2^K} \prod_{i=1}^N d_i^{\alpha K_i} \rho^{-K} \right)}{\log_{10} \rho} = K. \tag{18}$$

4. Numerical Results

We show the performance of the uplink cooperative system in LPWAN while varying the total received SNR (the effective SNR at the cloud server), which has three GWs ($N = 3$), each with the different number of the antennas. We also generalize for a distance from ID to each GW; i.e., $d_1 = 1$, $d_2 = 4$, and $d_3 = 8$.

Figure 2 shows the outage performances of uplink LPWAN with non-cooperative and cooperative techniques when $(K_1, K_2, K_3) \in \{(1, 3, 5)(5, 3, 1)\}$, $d_1 = 1$, $d_2 = 4$, $d_3 = 8$, $R = 1.5$, and $\alpha = 3$. In this figure, the analytic results derived from Equations (8) and (11), are exactly matched with the Monte-Carlo simulation results for all cases of antenna combination. They show that the cooperative technique always outperforms the non-cooperative technique. It also has better performances when the number of antennas of the near GW from the ID is more than the number of antennas of the far GW.

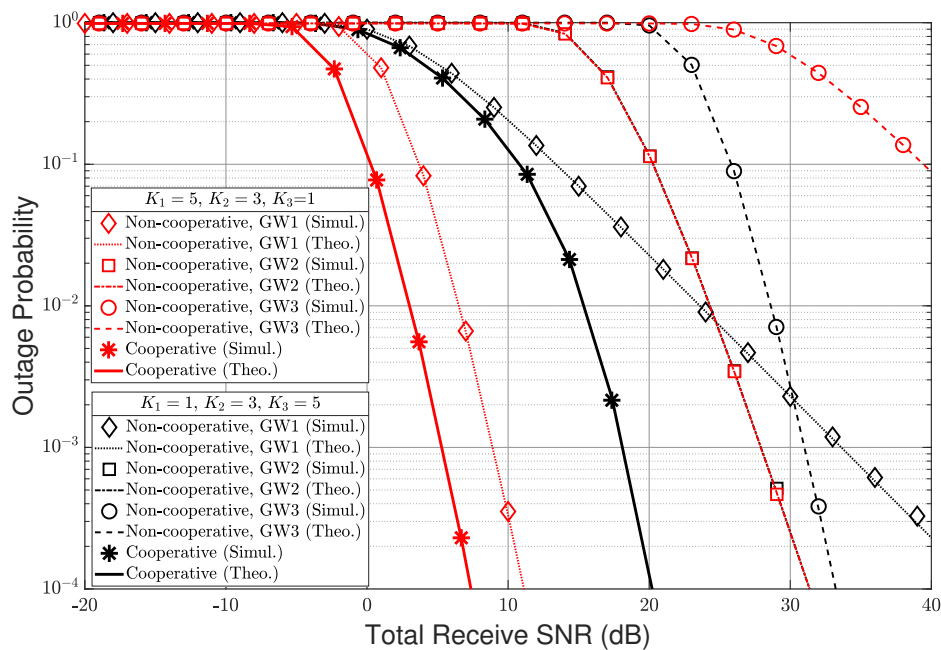


Figure 2. Outage probability performance of the LPWAN while varying the total received SNR when $N = 3$, $(K_1, K_2, K_3) \in \{(1, 3, 5)(5, 3, 1)\}$, $d_1 = 1$, $d_2 = 4$, $d_3 = 8$, $R = 1.5$, and $\alpha = 3$.

Figure 3 shows the BER performances on the same system as the simulation environment in Figure 2. The analyzed BER performances in this paper, Equation (13) and (15), are verified to match well with the simulation results by Monte-Carlo. The detailed interpretation of the results is omitted because it is the same as the interpretation of the result of outage probability.

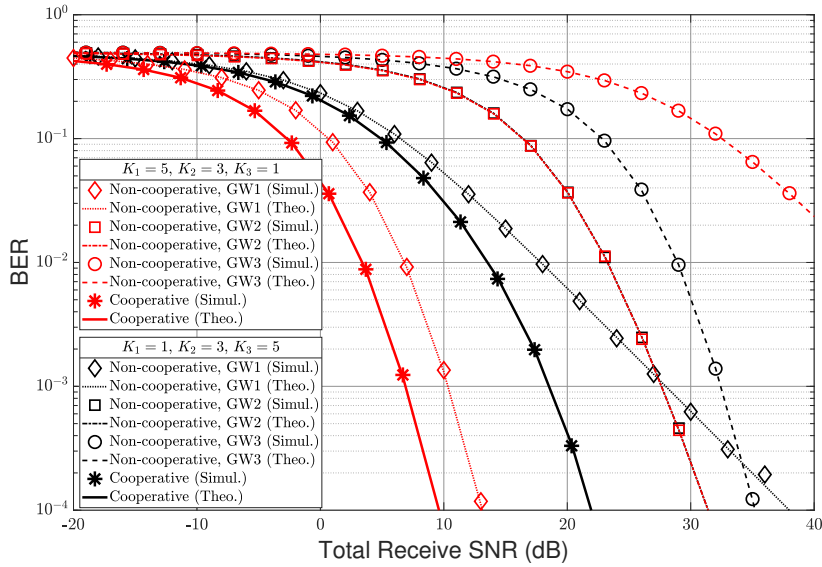


Figure 3. BER performance of LPWAN for varying the total received SNR when $N = 3$; i.e., $(K_1, K_2, K_3) \in \{(1, 3, 5)(5, 3, 1)\}$, $d_1 = 1$, $d_2 = 4$, $d_3 = 8$, and $\alpha = 3$.

Figure 4 validates the diversity order analysis of the uplink cooperative technique in LPWAN when $(K_1, K_2, K_3) \in \{(1, 3, 5)(5, 3, 1)\}$; i.e., $K = K_1 + K_2 + K_3 = 9$. As expected in Section 3.3, the asymptotic analysis results (17) are matched well with the exact analysis results in the form of an upper boundary curve as the SNR increases.

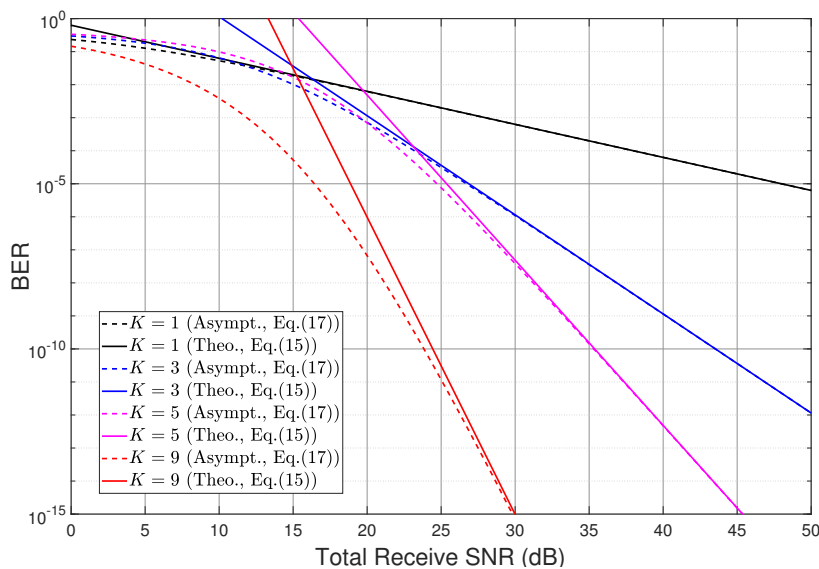


Figure 4. Diversity order of LPWAN according to the number of total received antennas when $d_1 = 1$, $d_2 = 3$, and $d_3 = 5$.

5. Conclusions

In this paper, the performance of a cooperative low-power wide-area network (LPWAN) was analyzed in terms of outage probability, bit error rate (BER), and diversity order, while there existed

N gateways (GWs) with multiple antennas. Despite the assumption that each GW is independently located at an arbitrary position and has an arbitrary number of antennas, we attained the exact closed-form expression on both outage probability and BER by using the hyper-Erlang distribution. It was shown that the mathematical analyses provided in this paper exactly matched with Monte-Carlo computer simulations, and thus the analytical results were validated. We investigated the diversity order of the cooperative LPWAN and verified that it is equal to the total number of received antennas in cooperative LPWANs via both mathematical analysis and computer simulations. As expected, the performance of cooperative LPWAN outperforms conventional non-cooperative LPWAN. Consequently, the cooperative LPWAN architecture is very promising for reducing the costs, extending the coverage ranges, and enhancing the battery lives of IoT devices.

Author Contributions: Formal analysis, C.S.Y.; investigation, C.S.Y. and J.S.Y.; methodology, C.S.Y.; project administration, B.C.J.; resources, B.C.J.; software, J.S.Y.; supervision, B.C.J.; validation, J.S.Y. writing—original draft, C.S.Y.; writing—review and editing, J.S.Y. and B.C.J. All authors have read and agreed to the published version of the manuscript.

Acknowledgments: This work was supported in part by the ICT R&D program of MSIT/IITP (2019-0-00964-001, Development of Incumbent Radio Stations Protection and Frequency sharing Technology through Spectrum Challenge), and in part by the MSIT (Ministry of Science and ICT), Korea, under the ITRC (Information Technology Research Center) support program (IITP-2020-2017-0-01635) supervised by the IITP (Institute for Information and communications Technology Promotion).

Conflicts of Interest: The authors declare no conflict of interest.

Abbreviations

The following abbreviations are used in this manuscript:

LPWAN	Low-power wide-area network
BER	Bit error rate
MRC	Maximum-ratio combining
IoT	Internet of Things
LTE	Long-term evolution
LTE-MTC	LTE machine-type-communications
NB-IoT	Narrow band-IoT
LoRa	Long range
BLE	Bluetooth low energy
mMTC	Massive machine-type-communications
GW	Gateway
RRH	Remote radio head
SNR	Signal-to-noise ratio
CDI	Channel distribution information
ID	IoT device
AWGN	Additive white Gaussian noise
p.d.f.	Probability density function
c.d.f.	Probability distribution function
QPSK	Quadrature phase-shift keying

The following mathematical symbols and functions are used in manuscript:

N	The total number of GWs that participate in the cooperative communication
K_i	The total number of antennas of i -th GW
K	The total sum of antennas of all GWs that participate in the cooperative communication
d_i	The distance between ID and i -th GW
α	Path loss factor
$\Gamma(\cdot)$	The gamma function
${}_2F_1(\cdot)$	The Gaussian hyper-geometry function

Appendix A. Hyper-Erlang Distribution

The hyper-Erlang distribution is the distribution of the sum of two or more independent Erlang random variables. In [15], the p.d.f. of hyper-Erlang distribution is given as

$$f_Z(z) = \sum_{i=1}^N \sum_{j=1}^{K_i} A_{ij} f_{Z_{\gamma_i}^j}(z) = \sum_{i=1}^N \sum_{j=1}^{K_i} A_{ij} \frac{(\gamma_i^{-1}z)^{j-1} \gamma_i^{-1}}{(j-1)!} e^{-\gamma_i^{-1}z}, \tag{A1}$$

where $f_{Z_{\gamma_i}^j}(z)$ is the p.d.f. of the Erlang distribution with $j\gamma_i$ mean and $j\gamma_i^2$ variance for RV $Z_{\gamma_i}^j$. The term A_{ij} is obtained by the recursive way in [19] as follows:

$$A_{ij} = \left(\frac{\prod_{t=1}^N \gamma_t^{-K_t}}{\gamma_i^{-j} (K_i - j)!} \right) \lim_{s \rightarrow -\gamma_i^{-1}} g_i^{(K_i - j)}(s), \tag{A2}$$

where $g_i^{(q)}(s)$ denotes the q -th derivative of $g_i(s) = \prod_{t=1, t \neq i}^N \frac{1}{(s + \gamma_t^{-1})^{K_t}}$. It is obtained iteratively as $g_i^{(q)}(s) = \sum_{l=0}^{q-1} \left[(q-l) (-1)^{l+1} \left(\sum_{t=1, t \neq i}^N \frac{(l)! K_t}{(s + \gamma_t^{-1})^{l+1}} \right) g_i^{(q-1-l)}(s) \right]$ for $q \geq 1$, where $g_i^{(0)}(s) = g_i(s)$.

Appendix B. The Taylor Expansion of P_b

The derived expression of P_b is composed of N variable terms which are polynomials. If we have the Taylor series for $f(x)$ and $g(x)$ which are polynomial, we can easily figure out the Taylor series for $f(x) + g(x)$, $f(x)g(x)$, and $f(x)/g(x)$ by just adding, multiplying, and dividing the series.

The coefficient A_{ij} can be considered with a more simple modified form for computation, given in [15,19]. It can be rewritten as follows

$$A_{i,K_i} = \prod_{t=1, t \neq i}^N \left(1 - \frac{\gamma_i^{-1}}{\gamma_t^{-1}} \right)^{-K_t} = \prod_{t=1, t \neq i}^N \left(1 - \frac{d_i^\alpha}{d_t^\alpha} \right)^{-K_t}, \tag{A3}$$

and for $j = K_i - 1$, down to 1, A_{ij} can be written as

$$A_{ij} = \frac{1}{K_i - j} \sum_{l=1}^{K_i - j} \left[A_{i,j+l} \sum_{p=1, p \neq i}^N K_p \left(1 - \frac{\gamma_i^{-1}}{\gamma_p^{-1}} \right)^{-l} \right] = \frac{1}{K_i - j} \sum_{l=1}^{K_i - j} \left[A_{i,j+l} \sum_{p=1, p \neq i}^N K_p \left(1 - \frac{d_i^\alpha}{d_p^\alpha} \right)^{-l} \right]. \tag{A4}$$

It certainly has a constant value without respect to ρ .

With Taylor expansion, $\sum_{j=1}^{K_i} A_{ij} P_b(i, j)$ can be derived as follows

$$\begin{aligned} \sum_{j=1}^{K_i} A_{ij} P_b(i, j) &= \sum_{j=1}^{K_i} \frac{A_{ij}}{2} (2j) \frac{{}_2F_1\left(1, 1/2 + j; 1 + j; \frac{2d_i^\alpha}{2d_i^\alpha + \rho}\right)}{\sqrt{\left(1 + \frac{2d_i^\alpha}{\rho}\right) \left(\frac{2\rho}{d_i^\alpha} + 4\right)^j}} \\ &= \sum_{j=1}^{K_i} \left(\frac{A_{ij}}{2} (2j) \sum_{r=0}^{\infty} \frac{\frac{\Gamma(1+r)\Gamma(1/2+j+r)\Gamma(1+j)}{\Gamma(1/2+j)r\Gamma(1+j+r)} \left(\frac{2d_i^\alpha}{2d_i^\alpha + \rho}\right)^r}{\sqrt{1 + \frac{2d_i^\alpha}{\rho} \left(\frac{2\rho}{d_i^\alpha} + 4\right)^j}} \right) \\ &\approx \sum_{j=1}^{K_i} \sum_{r=1}^{\infty} \left(A_{ij} \frac{(-1)^{r+1}}{2^{r+j-1}} \binom{2r+2j-3}{r+j-2} \binom{r+j-2}{j-1} d_i^{\alpha(r+j-1)} \rho^{-(r+j-1)} \right), \end{aligned} \tag{A5}$$

where ${}_2F_1$ indicates the Gaussian hyper-geometry function. Let a function $\beta_i(r, j)$ be defined as follows

$$\beta_i(r, j) = \begin{cases} A_{ij} \frac{(-1)^{r+1}}{2^{r+j-1}} \binom{2r+2j-3}{r+j-2} \binom{r+j-2}{j-1} d_i^{\alpha(r+j-1)}, & \text{if } r > 0 \\ 0, & \text{otherwise} \end{cases}, \tag{A6}$$

which denotes the coefficient of the r -th term in the j -th polynomial in (A5). Then, (A5) can be simply collected in a single indeterminate ρ as follows

$$\sum_{j=1}^{K_i} \sum_{r=1}^{\infty} \beta_i(r, j) \rho^{-(r+j-1)} = \sum_{r=1}^{K_i} \sum_{t=1}^r \beta_i(t, r+1-t) \rho^{-r} + \sum_{r=K_i+1}^{\infty} \left(\sum_{t=r-K_i+1}^r \beta_i(t, r+1-t) \rho^{-r} \right). \quad (A7)$$

Let $\beta_{i,r}$ be the coefficient of ρ^{-r} for the i -th variable term, which is given by

$$\beta_{i,r} = \begin{cases} \sum_{t=1}^r \beta_i(t, r+1-t) & \text{if } 1 < r \leq K_i \\ \sum_{t=r-K_i+1}^r \beta_i(t, r+1-t) & \text{if } r > K_i \end{cases}. \quad (A8)$$

Since the derived expression of P_b is composed of N polynomials, the sum of the Taylor series for all the polynomials is considered, of which all the coefficient of ρ^{-r} for $r < K$ are added to be zero.

$$\sum_{i=1}^N \beta_{i,r} = 0 \quad \text{for } r < K. \quad (A9)$$

Consequently, K -th term remains as the first-order term as follows.

$$\begin{aligned} P_b &= \sum_{i=1}^N \sum_{j=1}^{K_i} A_{ij} P_b(i, j) \\ &= \sum_{j=1}^{K_1} A_{1,j} P_b(1, j) + \sum_{j=1}^{K_2} A_{2,j} P_b(2, j) \dots + \sum_{n=1}^{K_N} A_{N,j} P_b(N, j) \\ &\approx \left(\sum_{i=1}^N \sum_{t=K-K_i+1}^K \beta_i(t, K+1-t) \right) \rho^{-K} + N\mathcal{O}(\rho^{-(K+1)}) \\ &= \left(\frac{\binom{2K-1}{K-1}}{2^K} \prod_{i=1}^N d_i^{\alpha K_i} \right) \rho^{-K} + N\mathcal{O}(\rho^{-(K+1)}) \\ &= \left(\frac{\Psi}{2^K} \prod_{i=1}^N d_i^{\alpha K_i} \right) \rho^{-K} + N\mathcal{O}(\rho^{-(K+1)}), \end{aligned} \quad (A10)$$

where $K = \sum_{i=1}^N K_i$.

References

- 3GPP TR 45.820, Cellular System Support for Ultra-Low Complexity and Low Throughput Internet of Things (IoT) v13.1.0. Available online: https://3gpp.org/ftp/Specs/archive/45_series/45.820 (accessed on 11 April 2019).
- Sornin, N.; Luis, M.; Eirich, T.; Kramp, T.; Hersent, O. LoRaWAN Sepcification. Available online: <https://loro-alliance.org/resource-hub/lorawanr-specification-v10> (accessed on 11 April 2019).
- Bluetooth SIG, Specification of the Bluetooth System, Core Specification. Available online: <https://www.bluetooth.com/specifications/bluetooth-core-specification/> (accessed on 11 April 2019).
- Qin Z.; Li, F.Y.; Li, G.Y.; McCann, J.A.; Ni, Q. Low-Power Wide-Area Networks for Sustainable IoT. *IEEE Wireless Commun.* **2019**, *26*, 140–145. [CrossRef]
- Barriquello, C.H.; Bernardon, D.P.; Canha, L.N.; Soares e Silva, F.E.; Porto, D.S.; da Silveira Ramos, M.J. Performance assessment of a low power wide area network in rural smart grids. In Proceedings of the 52nd International Universities Power Engineering Conference (UPEC), Heraklion, Greece, 28–31 August 2017.
- Mikhaylov, K.; Petaejaevaervi, J.; Haenninen, T. Analysis of Capacity and Scalability of the LoRa Low Power Wide Area Network Technology. In Proceedings of the 22th European Wireless Conference, Oulu, Finland, 18–20 May 2016.

7. Ochoa, M.N.; Guizar, A.; Maman, M.; Duda, A. Evaluating LoRa energy efficiency for adaptive networks: From star to mesh topologies. In Proceedings of the IEEE 13th International Conference on Wireless and Mobile Computing, Networking and Communications (WiMob), Rome, Italy, 9–11 October 2017.
8. Vejlgaard, B.; Lauridsen, M.; Nguyen, H.; Kovacs, I.Z.; Mogensen, P.; Sorensen, M. Coverage and Capacity Analysis of Sigfox, LoRa, GPRS, and NB-IoT. In Proceedings of the IEEE 85th Vehicular Technology Conference (VTC Spring), Sydney, Australia, 4–7 June 2017.
9. Gambiroža, J.Č.; Mastelić, T.; Šolić, P.; Čagalj, M. Capacity in LoRaWAN Networks: Challenges and Opportunities. In Proceedings of the 4th International Conference on Smart and Sustainable Technologies (SpliTech), Split, Croatia, 18–21 June 2019.
10. Bembe, M.; Abu-Mahfouz, A.; Masonta, M.; Ngqondi, T. A survey on low-power wide area networks for IoT applications. *Telecommun. Syst.* **2019**, *71*, 249–274. [[CrossRef](#)]
11. Centenaro, M.; Vangelista, L.; Zanella, A.; Zorzi, M. Long-range communication in unlicensed bands: The rising starts in the IoT and smart city scenarios. *IEEE Wireless Commun.* **2016**, *23*, 60–67. [[CrossRef](#)]
12. Finnegan, J.; Brown, S. An Analysis of the Energy Consumption of LPWA-based IoT Devices. In Proceedings of the 2018 IEEE International Symposium on Networks, Computers and Communications (ISNCC), Rome, Italy, 19–21 June 2018.
13. Dongare, A.; Narayanan, R.; Gadre, A.; Luong, A.; Balanuta, A.; Kumar, S.; Iannucci, B.; Rowe, A. Charm: Exploiting Geographical Diversity through Coherent Combining in Low-Power Wide-Area Networks. In Proceedings of the 2018 17th ACM/IEEE International Conference on Information Processing in Sensor Networks (IPSN), Porto, Portugal, 11–13 April 2018.
14. Khan, F.A.; He, H.; Xue, J.; Ratnarajah, T. Performance Analysis of Cloud Radio Access Networks with Distributed Multiple Antenna Remote Radio Heads. *IEEE Trans. Signal Process.* **2015**, *63*, 4784–4799. [[CrossRef](#)]
15. Kadri, T.; Smaili, K. Convolutions of Hyper-Erlang and of Erlang Distributions. *Int. J. Pure Appl. Math.* **2015**, *98*, 81–89. [[CrossRef](#)]
16. Georgiou, O.; Raza, U. Low Power Wide Area Network Analysis: Can LoRa Scale? *IEEE Wireless Commun. Lett.* **2017**, *6*, 162–165. [[CrossRef](#)]
17. Tse, D.; Viswanath, P. *Fundamentals of Wireless Communication*; Cambridge University Press: Cambridge, UK, 2005.
18. Yeom, J.S.; Jang, S.J.; Ko, K.S.; Jung, B.C. BER Performance of Uplink NOMA with Joint Maximum-Likelihood Detector. *IEEE Trans. Veh. Technol.* **2019**, *68*, 10295–10300. [[CrossRef](#)]
19. Kadri, T.; Smaili, K. The Exact Distribution of the Ratio of Two Independent Hypoexponential Random Variables. *Br. J. Math. Comput. Sci.* **2014**, *4*, 2665–2675. [[CrossRef](#)]



© 2020 by the authors. Licensee MDPI, Basel, Switzerland. This article is an open access article distributed under the terms and conditions of the Creative Commons Attribution (CC BY) license (<http://creativecommons.org/licenses/by/4.0/>).